

CFD Jet Mixing Model Validation against Zero-Boil-Off Tank (ZBOT) Microgravity Experiment

O. Kartuzova and M. Kassemi
National Center for Space Exploration Research (NC SER)
NASA Glenn Research Center
Cleveland, OH 44135

A CFD model for simulating the fluid dynamics of the jet induced mixing process is utilized in this paper to model the jet mixing portion of the Zero Boil-Off Tank (ZBOT) experiment in microgravity [1]. The Volume of Fluid (VOF) method is used for modeling the dynamics of the interface during mixing. The simulations were performed at different jet speeds and liquid fill levels. The effects of the jet angle and orientation, values of gravitational acceleration and surface tension, as well as the discretization scheme used with the volume fraction equation on the jet-ullage interaction were studied and discussed in this paper. The computational results for the jet-ullage interaction are compared with images taken during the experiment. A qualitative comparison shows that the CFD model was able to capture the main features of the interfacial dynamics, as well as the jet penetration of the ullage at different jet speeds and liquid fill levels.

Nomenclature

E	= Energy	<u>Greek</u>	
\mathbf{g}	= Gravity	α	= Cell value of volume fraction
h	= Surface curvature	μ	= Dynamic viscosity
n	= Normal vector	ρ	= Density
p, P	= Pressure	<u>Subscripts</u>	
t	= Time	q	= Interface or phase
\mathbf{v}	= Velocity		

I. Introduction

The cost of development and the risk of operations for future NASA exploration missions employing in-space cryogenic storage and transfer systems can be significantly reduced by improving the capability of the Computational Fluid Dynamics (CFD) models that provide predictive simulations of the two-phase fluid dynamics and heat transfer phenomena that govern the performance of the propellant and life support systems in settled and unsettled states. The development and validation of the CFD models against both full scale cryogenic ground-based experiments (settled conditions) and subscale micro-g flight data (unsettled conditions) forms an integral part of the NASA Evolvable Cryogenics project (eCryo). The purpose of the present study is to assess the ability of the current two-phase CFD models to predict the fluid dynamics of jet-induced mixing in microgravity, which is aligned with the goals of the eCryo project.

The Zero-Boil-Off Tank (ZBOT) experiments are a series of small scale fundamental science experiments aboard the International Space Station (ISS) that use a transparent volatile simulant fluid in a transparent sealed tank to delineate various fluid flow, heat and mass transport, and phase change phenomena that control storage tank pressurization and pressure control in microgravity [1]. The hardware for ZBOT-1, the first of three envisioned hierarchical experiments is shown in Fig 1. The hardware payload flew to the ISS on the OA-7 flight on April 18th, 2017, and operations were initiated in September 2017. The experiment lasted roughly 3 months and encompassed more than 90 tests which studied fluid flow and thermal stratification during the self-pressurization interval, as well as thermal de-stratification, depressurization, mixing and jet ullage penetration dynamics during the pressure control interval. Hand-in-hand with the experiments, a comprehensive two-phase Computational Fluid Dynamics (CFD) model was also developed for simulating and predicting pressure control. The model uses a VOF interface capturing scheme [2] to predict the interfacial dynamics and evolution of fluid velocities in the liquid and vapor phases. The objective of the present study is to assess the ability of the ANSYS Fluent CFD code to accurately predict jet mixing in microgravity by comparing CFD results with the extensive microgravity data provided by the ZBOT experiments.

Previous experimental and computational studies of jet mixing for the purpose of propellant pressure control are limited in number. Some early experimental work was done by Aydelott [3]. He studied the liquid flow patterns that result from the axial-jet mixing of ethanol in 10-cm-diameter containers under zero-, reduced-, and normal-gravity conditions in an experimental program conducted in the Lewis Research Center's zero-gravity facility. This experimental study was accompanied by a modeling effort. These results, though significant, are limited by the short duration of the experiment which was directed by the nature of the microgravity environment that was used. The Tank Pressure Control Experiment (TPCE) is another experiment that studied effects of jet mixing in microgravity. This experiment flew on the Space Shuttle in 1991 (STS-43). The objectives of TPCE included characterizing the fluid and interface dynamics during jet mixing in microgravity, and providing data for use in the validation of CFD models of storage tanks under unsettled conditions [4]. The experiment utilized a small scale transparent cylindrical tank, partially filled with a simulant fluid (Freon-113). Two heaters were installed inside the tank for the tank self-pressurization experiments, one at the top of the dome opposite the nozzle, and one at the center of the tank near the wall. A pump drew liquid out of the tank through a liquid acquisition device (LAD) and returned it via an axial jet during the tank pressure control tests. Video recording of the tank was conducted in order to capture the ullage dynamics; however, due to data storage limitations, only the first 2 minutes of each tank self-pressurization test and the first 4 minutes of each jet mixing test were recorded. Computational work related to TCPE was performed by Wendl et al. [5], Breisacher and Moder [6] and Kartuzova and Kassemi [7]. Wendl et al. [5] examined the formation of geysers by an axial jet using a 2D CFD code prior to the experiment's operation. Breisacher and Moder studied the ullage dynamics that occurred during the TPCE pressure control experiments utilizing the Flow3D CFD code. Kartuzova and Kassemi performed a similar study using the ANSYS Fluent CFD code. In the latter studies, the jet penetration of the ullage was correctly captured by the models, and the ullage shapes and dynamics, as well as the final equilibrium position of the ullage, were qualitatively reproduced [6,7]. A drawback of the TPCE experiment was that the heaters were located inside the tank, and therefore possibly affected jet-ullage interaction during mixing, for example by pinning the ullage during the impingement of the jet on the surface of the interface.

The main focus of the present work is to model ZBOT jet mixing tests 9, 24, 27, 260, 254 and 258 using the Volume of Fluid (VOF) model of the ANSYS Fluent CFD code, and to validate the two phase CFD model against the experimental results. The details of the test runs that were used to validate the model are summarized in Table 1.

Table 1: Details of computational cases

<i>Jet Speed</i>	<i>Fill Level: 70%</i>	<i>Fill Level: 90%</i>
4 cm/s		260
6 cm/s	9	
10 cm/s	24	254
25 cm/s	27	258

II. Mathematical Model

A. Governing Equations

The fluid flow and heat transfer in the tank are described in terms of the continuity, Navier-Stokes, and energy equations for both phases:

$$\frac{\partial \rho}{\partial t} + \nabla(\rho \mathbf{v}) = 0, \quad (1)$$

$$\frac{\partial}{\partial t}(\rho \mathbf{v}) + \nabla(\rho \mathbf{v} \mathbf{v}) = -\nabla p + \nabla[\mu_{eff}(\nabla \mathbf{v} + \nabla \mathbf{v}^T)] + \rho \mathbf{g} + \mathbf{F}_{vol}, \quad (2)$$

$$\frac{\partial}{\partial t}(\rho E) + \nabla(\mathbf{v}(\rho E + p)) = \nabla(k_{eff} \nabla T) + S_h. \quad (3)$$

In the present study, the liquid phase is treated as incompressible. The vapor is modeled as a compressible ideal gas. All of the thermophysical and thermodynamic properties of the fluids are taken from the DIPPR database [8-11] at saturation conditions.

The primary focus of this study is to capture the main dynamics of the fluid flow and jet-ullage interactions. Therefore, although the energy equation was solved, all of the walls were treated as adiabatic, and any phase change mass transfer between the liquid and vapor phases was not considered. The movement of the interface is captured diffusely using the Volume of Fluid (VOF) method, as promulgated by Hirt and Nichols [2]; this method is described below.

B. VOF Model

In the VOF method, a volume fraction is defined in each cell such that the volume fractions of all of the phases sum to unity. In each cell, the change in the interface can be tracked by solving a continuity equation for the volume fraction of the q^{th} phase:

$$\frac{1}{\rho_q} \left[\frac{\partial}{\partial t} (\alpha_q \rho_q) + \nabla \cdot (\alpha_q \rho_q \mathbf{v}_q) \right] = S_{\alpha_q}, \quad (4)$$

where the volume fraction for the primary phase is determined from:

$$\sum_{q=1}^n \alpha_q = 1. \quad (5)$$

In the VOF method, the field variables and properties are defined in terms of the volume fraction, which for a general system can be written as:

$$\rho = \sum_{q=1}^n \alpha_q \rho_q, \quad \mu_{eff} = \sum_{q=1}^n \alpha_q \mu_{eff,q}, \quad k_{eff} = \sum_{q=1}^n \alpha_q k_{eff,q}. \quad (6)$$

In this fashion, the continuity, momentum, and energy equations, as described by Eq. (1) – (3), can be solved throughout the domain for the temperatures and velocities in the two phases. In the VOF model, the energy (E) and temperature (T) are treated as mass-averaged variables:

$$E = \frac{\sum_{q=1}^n \alpha_q \rho_q E_q}{\sum_{q=1}^n \alpha_q \rho_q}, \quad (7)$$

where E_q is based on the specific heat of the q^{th} phase and the shared temperature.

In the present implementation, the surface tension forces at the interface are modeled via the Continuum Surface Force (CSF) model of Brackbill et al. [12]. In this model, the surface tension forces at the interface are transformed into a volume force (\mathbf{F}_{vol}), which is added as a source to the momentum equation:

$$\mathbf{F}_{vol} = \sum_{pairs\ i,j,i<j} \sigma_{ij} \frac{\alpha_i \rho_i h_i \nabla \alpha_j + \alpha_j \rho_j h_j \nabla \alpha_i}{\frac{1}{2}(\rho_i + \rho_j)}, \quad (11)$$

where h_i is the surface curvature calculated from the local gradients in the surface normal at the interface:

$$h_i = \nabla \cdot \hat{\mathbf{n}}. \quad (12)$$

C. Turbulence modeling

The Reynolds Averaged Navier–Stokes (RANS) approach to turbulence modeling was compared with the Large Eddy Simulation (LES) method for simulating jet mixing in the ZBOT experiment.

The Shear Stress Transport $k-\omega$ ($k-\omega$ -SST) RANS model of Menter [13] was utilized. This model is similar to the standard $k-\omega$ model of Wilcox [14], but has the ability to account for the transport of the principal shear stress in adverse pressure gradient boundary layers. The model is based on the assumption of Bradshaw et al. [15] that the principal shear stress is proportional to the turbulent kinetic energy, which is introduced into the definition of the eddy-viscosity. These features make the $k-\omega$ -SST model more accurate and reliable for a wider class of flows than the standard $k-\omega$ model. In the VOF model, the continuity of the turbulent quantities is inherently assumed since one set of equations for the turbulent kinetic energy and dissipation rate is solved for both phases throughout the domain, with the fluid properties varying according to the local volume fraction value.

In the LES model, large eddies are resolved directly while small eddies are modeled. In the current LES model, the Wall-Adapting Local Eddy-Viscosity (WALE) [16] sub-grid scale model is utilized for modeling the unknown stresses that result from the filtering operation.

III. Numerical Implementation

D. Tank Geometry

The experimental tank is made out of polished optical quality cast acrylic and is 4” in diameter and 8” tall. It consists of a cylindrical midsection capped at the two ends by hemispherical domes. It’s equipped with a strip heater mounted on the outer surface of the cylindrical acrylic wall, which is used to self-pressurize the tank. A nozzle located at the bottom is activated during the pressure control tests. A screened Liquid Acquisition Device (LAD) ensures that only liquid is extracted from the tank, which is then thermally conditioned and pumped in through the nozzle during the jet mixing cycles. To provide proper containment, as well as definable and controllable thermal boundary

conditions for model validation, the tank is isolated from the Microgravity Science Glovebox (MSG) environment via a temperature controlled Vacuum Jacket (VJ) that is, in turn, enclosed within another cooling jacket. The tank fluid temperature prior to each test and the jet flow temperatures during the mixing cycles are maintained by careful conditioning of the fluid via a counter-flow shell and tube heat exchanger in the Fluid Supply Unit (FSU) located just below the test cell in the MSG. The ZBOT test tank and experimental setup are shown in Fig. 1. For modeling jet mixing the ZBOT geometry was simplified. The reduced geometry included only the fluid inside the tank, reduced outlet tube and nozzle inlet, as shown in Fig. 2.

E. Initial Conditions

The ullage was initialized at the centerline of the tank with a 1 mm gap between the top of the ullage and the top of the tank. Several test runs were completed to allow the ullage to move to an initial location based on the gravitational acceleration data. However, the jet mixing simulations that were performed from this initial condition showed results very similar to the results of the cases where the ullage was initialized at the centerline of the tank. The ullage was initialized at the centerline of the tank for the majority of the cases reported here. In the cases with the RANS turbulence models initial values for turbulence kinetic energy and specific dissipation rate were set, respectively, to $1e-06 \text{ m}^2/\text{s}^2$ and 100 1/s . Even though the tank and fluid were nearly isothermal during mixing, the energy equation was solved for all cases. The tank temperature was initialized to a uniform value of 311.15 K prior to the beginning of jet mixing. Initial tank pressure was set to the saturation pressure at the initial tank temperature based on the DIPPR database.

F. Boundary Conditions

The tank wall was not included in calculations, an adiabatic boundary conditions were used on the outside of the fluid region. Since the cooling process is fast, this assumption is justified; nonetheless it can introduce some difficulty in predicting the measured temperature in the tank close to the wall, as will be discussed later. A contact angle between the liquid and the tank was assumed to be 0 degrees. A no slip boundary condition was applied on the inside of the tank wall which was in contact with fluid. Measured temperature and velocity evolutions were applied at the jet inlet in both RANS and LES cases. The Spectral Synthesizer condition [17] was used with the LES model to allow for random velocity (both magnitude and direction) fluctuations for more realistic inlet profile. Inlet jet angle of 5 deg. to the right in the ZBOT image taking view was applied, based on the insight from the particle streaking data, as will be discussed later. A shortened outlet tube was included in the geometry, with a velocity outlet B.C. used in a way in which mass flow rates at the inlet and outlet are matched for mass conservation.

G. Material Properties

In order to simulate cryogenic fluid, the ZBOT experiment used the refrigerant Perfluoro-n-Pentane (PnP, or C5F12), a nonpolar volatile fluid with a boiling point of $29 \text{ }^\circ\text{C}$ at 1 atm. and a near zero contact angle with the test tank. A high purity (99.7% straight-chained n-isomer) version of PnP was approved by NASA toxicology and ECLSS groups to be safe for use in the International Space Station (ISS). A small amount of Krytox was added to PnP to prevent DPIV particles from sticking to the surfaces of the tank. In the model, constant material properties were used for the PnP-Krytox mixture. The properties are summarized in Table 2.

Table 2. PnP-Krytox mixture properties at 311.15 K:

<i>Property</i>	<i>Units</i>	<i>PnP-Krytox liquid</i>	<i>PnP vapor</i>
<i>Density</i>	kg/m^3	1556.10763	Ideal gas
<i>C_p</i>	J/kg-K	1234.06729	793.70196
<i>Thermal Conductivity</i>	W/m-K	0.05786254	0.01059
<i>Viscosity</i>	$\text{Pa}\cdot\text{s}$	0.00040202864	1.1501234e-05
<i>Surface Tension</i>	N/m		0.0081136
<i>Molecular Weight</i>	kg/kmol		288.034

H. Computational mesh

Two different computational grids were used in the current study. They are shown in Fig. 2. The LES mesh and the RANS mesh were used for modeling LES and RANS cases respectively. These meshes, which consisted of all tetrahedral cells, were created in ANSYS Meshing and converted to polyhedral elements in ANSYS Fluent. Approximately 6 times reduction in size was achieved at every conversion. Grid sizes shown in Fig. 2 are for tetrahedral meshes before conversion.

I. Discretization and convergence

The Second Order Upwind scheme was used to discretize the momentum, energy, and turbulence equations (cell values). The PISO scheme was used for the pressure-velocity coupling (cell values). The Least Squares Cell Based scheme was used for the gradient calculations (face values). The PRESTO! scheme was used for the pressure interpolation (face values). The Point Implicit (Gauss-Seidel) linear equation solver with the Algebraic Multi-Grid (AMG) method was used to solve the linearized systems of equations. The First Order Implicit temporal discretization scheme was used with the explicit VOF model with a time step size equal to 0.01 seconds for RANS simulations and 0.0005 seconds for LES. The Geometric Reconstruction scheme was used to discretize the volume fraction equation. The convergence criteria are set to 1×10^{-4} for all of the equations except the energy equation, for which it is set to 1×10^{-6} .

IV. Results and Discussion

After reviewing the ZBOT experimental results several cases were selected for modeling jet mixing phenomena. These cases had a minimal amount of bubbles in the tank, and didn't have boiling of any kind during the initial mixing and therefore were considered "clean" and appropriate for modeling. These cases are summarized in Table 1 above. Grid and time step size independence studies were completed for case 254 with heat and mass transfer. It is assumed that if the results are grid independent for a case with phase change, they would also be grid independent for a jet mixing only case without phase change. The results of the cases with phase change, including the results of the grid and time step size independence studies, are not presented in this paper, they will be published later. The grids used in this paper for both LES and RANS simulations were proven to be grid independent.

Prior to conducting model validation against the ZBOT jet mixing experiments, a number of parametric studies was completed to study the effects of different physical and numerical factors on jet-ullage interaction. These factors include jet orientation and the value of the jet angle, the value of gravitational acceleration, the value of surface tension, and discretization scheme used for the volume fraction equation. The results of these studies are presented in this paper, since they are considered to be valuable information for understanding details of modeling mixing in microgravity.

J. Results of parametric studies

The effect of the discretization scheme used with the volume fraction equation

The effect of the discretization scheme for the volume fraction equation was studied and results are presented here. Three different discretization schemes which are available in ANSYS Fluent were considered: Geometric Reconstruction, Compressive and Modified HRIC. The descriptions of these discretization schemes can be found in ANSYS Fluent Theory Guide [17], and therefore are not repeated here. The effect of the discretization scheme for the volume fraction equation on the ullage shape and position was studied using ZBOT case 256. The ullage shapes that are predicted using these schemes are compared to the experimental white light image in Fig. 3. Since the shape and position of the ullage didn't change much after the initial adjustment, the CFD results were compared to the experimental image after 40 seconds of mixing. At this time in the experiment, as can be seen in Fig. 3, the ullage stays at the top of the tank on the left side. The results of the Geometric Reconstruction, Compressive, and Modified HRIC discretization schemes with the CFD RANS model are presented in the form of phase distribution in Fig. 3. All three discretization schemes resulted in ullage moving down towards the nozzle on the left side of the tank. The Geometric Reconstruction scheme predicted the sharpest interface and the ullage shape which is the best agreement with the experimental data. The Compressive scheme resulted in a somewhat diffused interface, while the Modified HRIC scheme predicted a much diffused interface.

The results of the Geometric Reconstruction and Compressive schemes used with the LES model after 23 seconds of mixing are presented in Fig. 4. This figure shows that the Geometric reconstruction scheme is superior to the Compressive scheme in predicting the interface shape and position which are in better agreement with the experimental data when used with the LES model.

Based on the results of this study it was decided to use the Geometric Reconstruction scheme for the volume fraction equation for validating all ZBOT mixing cases.

The effect of jet orientation

As it was observed in the experimental DPIV streaking images and will be discussed later in this paper, the jet in the experiment seems to be tilted. It seems that a tilt of 5 degrees to the right in the experimental view plane is a reasonable assumption. However, since only one view is available from the experiment it is very difficult to tell if

the jet was tilted relative to the ZBOT view plane. Due to this uncertainty a parametric CFD study with jet orientations varying in the ZBOT view plane and in the plane normal to the ZBOT view plane was conducted. The results of a study with the RANS model for ZBOT case 256 are presented here. Of course, the jet in the experiment could be tilted in planes other than the ZBOT view plane or a plane normal to it, however it is not possible to investigate all possible combinations. The jet angle combinations studied include:

- 1) 5 degrees to the right
- 2) 5 degrees to the front
- 3) 5 degrees to the front and 5 degrees to the right
- 4) 5 degrees to the back and 5 degrees to the right.

Jet tilting to the left in the ZBOT plane was not considered because it is clear from the experimental images that the tilt is to the right. The results of the cases with the jet orientations 1-4 are compared with the experimental image in Fig. 5. The results indicate that the 5 degrees angle to the right jet orientation produces the ullage position closest the experimental one, therefore this jet orientation was used in all ZBOT jet mixing simulations.

The effect of jet angle value

The effect of the jet angle value on the jet-ullage interaction was studied with the ZBOT case 9. Three different values of jet angle: 1, 2 and 5 degrees were considered. The results of the cases ran with these three different jet angle values are presented in Fig. 6. In the experimental case 9 the ullage moved down towards the nozzle and began hovering close to the nozzle within the first minute of mixing. The only CFD case that produced the results close to the experimental observations is the case with 5 degrees jet angle in which the ullage moved close to the nozzle within the first 100 seconds of mixing. In the other two cases the ullage also moved down towards the nozzle, however the speed of this movement was much slower than in the experiment. Therefore, a jet angle value of five degrees was selected for completing the ZBOT jet mixing validation studies.

The effect of the value of gravitational acceleration

Quasi-steady gravitational acceleration was not measured for the whole duration of the ZBOT experiment due to a failure of the Microgravity Acceleration Measurement System (MAMS). Instead, time shifted historical MAMS data (nominal) was used as an input for gravitational acceleration for model validation. This approach seemed to work well, however, a need for a study of the effect of gravitational acceleration on the jet-ullage interaction is justified. This study was conducted using ZBOT case 256, where the results of a case using the nominal value of gravitational acceleration are compared with the results of a case with 10 times the nominal value. The results of these two cases are compared in Fig. 7, which shows no difference between these two cases. Therefore it can be concluded that varying gravitational acceleration an order of magnitude has little effect on the jet-ullage interaction.

The effect of the value of surface tension

The results of a case with a nominal value of surface tension (reported in Table 2) were compared with the results of a case with double the nominal value. The results of these two cases are compared in Fig. 8. In both cases the ullage moved down towards the nozzle which is different from its behavior in the experiment where it stayed at the top of the tank (see Figs. 3-5). The shape of the ullage predicted by the model with double the value of surface tension is more stretched and better resembles the shape of the ullage in the experiment, compared to the results of the cases with the nominal surface tension value. However, it is difficult to justify changing a property (surface tension) by so much without a very solid reason, therefore the nominal surface tension value was used in all of the ZBOT validation cases.

K. Results of ZBOT jet mixing validation cases

Case 9: 70% fill, 6 cm/s jet speed

ZBOT Case 9 was modeled first with a straight jet and the results for the ullage location were compared with the experimental data at the beginning and end of the simulation. Initial ullage location from the experiment and CFD are shown in Fig. 9. At this time the, ullage is centered at the top of the tank in both CFD and experiment. At the end of the CFD simulation, as shown in Fig. 10, the ullage remained at the same initial position, however, in the experiment it moved towards the nozzle. This discrepancy was difficult to explain at first, but after reviewing the flow in the experiment as revealed by the particle streaks, it was obvious that the jet flow is coming into the tank at an angle, as shown in Fig. 11. This angle is difficult to define, but values between 3 and 6 degrees seem reasonable. Value of 5 degrees was selected and case 9 was modeled with this value for the jet angle set as a boundary condition. The results at the end of this case are shown in Fig. 12. This time, the ullage came down in CFD, just as it did in the experiment.

Fig. 13 shows the pressure contours at the center plane of the tank for a straight and tilted 5 degrees to the right jets. The figure shows that, in both cases, a high pressure point is present in the location where the jet hits the ullage. However, in the case of the straight jet this high pressure point is located at the center line of the tank and does not result in any ullage movement. In the case of the tilted jet, however, the high pressure point is located off-center to the right from the tank center line. This asymmetrical position results in the movement of the ullage to the left and then the flow in the tank moves it further down towards the nozzle. Based on the results of this case and previously discussed parametric studies, it was decided to use a 5 degree jet angle for modeling all ZBOT cases.

Case 24: 70% fill, 10 cm/s jet speed

ZBOT Case 24 was modeled using the LES turbulence model. This case has a similar fill level as case 9, but has a higher jet speed of 10 cm/s. The ullage was initialized at the center axis near the top of the tank. Ullage positions from CFD and experiment and a center plane with curved vectors from CFD are shown in Fig. 14 at 1.6 seconds of mixing. Ullage shape predicted by CFD matches the experimental results very well. An indentation created by the jet is clearly visible at the center of the lower region of the interface in both CFD and experiment. At this time during mixing the ullage is located near the top of the tank. Ullage positions from CFD and experiment and a center plane with curved vectors from CFD are shown in Fig. 15 at 25.5 seconds of mixing. At this time the indentation is still present, but the ullage moved down from the top of the tank. The CFD results agree with the experimental data very well.

Case 27: 70% fill, 25 cm/s jet speed

ZBOT Case 27 was modeled using both the LES and RANS turbulence models. This case has a similar fill level to cases 9 and 24, but has the highest tested jet speed of 25 cm/s. The ullage was initialized at the center axis near the top of the tank. Figures 16-18 show comparisons between the LES model predictions and the experiment at 4.1, 19 and 35 seconds of mixing. Figs. 16-18 show good resemblance in ullage shape and position between CFD LES model predictions and the experiment for 4.1 and 35 seconds of mixing. At 19 seconds of mixing, as shown in Fig. 17, CFD LES model predicts more elongated ullage shape residing mostly on the left side of the tank, when in the experiment the ullage is more centered with the jet penetration clearly visible near the tank center line. This might indicate that the jet tilt angle in the experiment might be somewhat different from the value used here, or might be changing. Ullage positions and flow structures at the tank center plane are compared between CFD LES and RANS models results in Fig. 19 at 3.5 seconds of mixing. These cases were completed with the nominal jet velocity and jet tilted 5 degrees to the right and to the front. Experimental data for this test was recorded with a delay after beginning of mixing and not available for this time instance. Fig. 19 indicates that LES predicts similar ullage shape and on average similar jet flow structures as the RANS model. However, LES resolves more vortices in the jet flow and predicts deeper and more centered penetration, as compared to the results of the RANS model. As shown in Fig. 20, at 13.3 seconds of mixing the LES model predicts ullage shape and the depth of the jet penetration which resemble the experimental results much closer than the RANS model prediction. The LES model also predicts more ullage surface deformations (ripples), as compared to the RANS model, which compares better with the experiment.

Case 260: 90% fill, 4 cm/s jet speed

ZBOT case 260 was modeled using both LES and RANS models. This is a case with a higher fill level of 90%, as compared to the previously discussed cases. In all of the simulations using the jet speed of $1.35 \cdot V_{\text{nominal}}$ the ullage stayed at the top of the tank; however, in the experiment the ullage moved down towards the nozzle during mixing. The 1.35 factor for jet velocity was used to account for the nozzle area blockage by debris. However, when ZBOT hardware was disassembled on the ground, it was observed that about half of the screen inside the nozzle was clogged by debris, as shown in Fig. 21. This means that the open area of the nozzle was reduced by 50% and, therefore, the jet velocity doubled. Two simulations, laminar and LES, were completed with $V \cdot 2$ and open area of the nozzle reduced by 50%. The initial ullage positions from CFD and the experiment are shown in Fig. 22. Ullage positions after 60 seconds of mixing are compared between the LES and laminar CFD cases and the experiment in Fig. 23. Ullage stayed at the top of the tank in the laminar case, however, it came down in the LES case. The LES case with $V \cdot 2$ matched the experimental data for ullage position much better than any other cases ran, including the LES case with $V \cdot 1.35$, however, there is still a difference in ullage position between this case and the experiment. In the experiment, as shown in Fig. 23, the ullage moved towards the center of the tank, while in the LES $V \cdot 2$ case it is on the left side of the tank. This might indicate that the jet angle in the experiment could be somewhat different from what was used in CFD, however, the exact jet angle from the experiment is impossible to identify.

Case 254: 90% fill, 10 cm/s jet speed

ZBOT case 254 was modeled using CFD LES and RANS models. This case has a similar fill level as ZBOT case 260, but higher jet speed of 10 cm/s. Jet flow structures and ullage positions are compared between the two models and the experiment in Figs. 24 and 25 at 20 and 120 seconds after beginning of mixing respectively. As can be seen in Fig. 24, the LES model predicts ullage coming down from the top and to the right side of the tank, which is in a much better agreement with the experiment at 20 seconds of mixing compared to the results of the RANS model. The RANS model predicts that ullage remains higher and on the left side of the tank. The jet flow structures are much better resolved in the LES simulation and compare well with the streak lines obtained from processing the experimental DPIV data. Fig. 25 shows similar comparison between the LES and RANS models and the experiment at 120 seconds of mixing. At this time the LES model is also in a better agreement with the experimental ullage shape and location, as well as the flow structures produced by the jet, as compared to the RANS model.

Case 258: 91.78% fill, 25 cm/s jet speed

ZBOT Case 258 was simulated using the CFD LES model. This case has a fill level similar to ZBOT cases 260 and 254, but jet speed of 25 cm/s, which is the highest speed studied. Two different jet speeds (to account for a different possible amount of nozzle blockage with debris) are compared in this case, just like in the case 260. Initial ullage positions from CFD and experiment are shown in Fig. 26. In the experiment the ullage is located slightly to the left from the tank axis, while in CFD it is centered. The jet flow structures and ullage positions predicted by the CFD LES models with $V^*1.35$ and V^*2 are compared with the experimental data in Fig. 27 at 51.5 seconds of mixing. At this time the model with V^*2 predicts ullage shape and position which are in a better agreement with the experimental ones, as compared to the results of the model using $V^*1.35$. The model with $V^*1.35$ predicts that the ullage has moved lower towards the center of the tank at 51.5 seconds of mixing, while in the experiment it stayed at the top.

V. Conclusion

Two-phase flow simulations of jet mixing in microgravity were conducted using storage tank CFD model in the framework of the ANSYS Fluent CFD code. The model results were validated against the results of the Zero Boil-Off Tank (ZBOT) jet mixing experiments in microgravity. The simulations were performed for different liquid fill levels and jet speeds.

A number of parametric and sensitivity studies were performed to check the various aspects of the model for simulating the experiment. These studies aided in the understanding of the effects of varying several parameters on the jet-ullage interaction. These parameters include: 1) jet orientation; 2) value of jet angle; 3) value of residual gravity; 4) value of surface tension; and 5) discretization scheme for the volume fraction equation. While the jet angle and orientation, and the surface tension had significant effects on the jet-ullage interaction, varying the value of the residual gravity by an order of magnitude didn't seem to have much effect. Geometric reconstruction discretization scheme for the volume fraction equation proved to be superior to the other studied schemes in predicting the correct ullage shape and position and produced the sharpest interface. Based on this parametric analysis final configurations of the model were decided.

The ullage shape and position were compared with the experimental data in six modeled ZBOT test runs. The fidelity of the model was assessed for different turbulence approaches. In addition to the laminar model, both the Reynolds Averaged Navier-Stokes (RANS) and the Large Eddy Simulation (LES) turbulence models were used, and the results for all three models were compared to the experimental data. The LES model was able to accurately predict the ullage shape and position in all cases considered, with the best agreement in the cases with the medium jet speed (10 cm/s). The RANS model did not predict the dynamic behavior of the ullage movement and its deformation with the same fidelity as the LES model. In summary, the results of the simulations showed that the LES approach to turbulence modeling is superior to RANS in predicting ullage movement and deformation during initial mixing. However, the disadvantage of the LES approach is that it requires significantly larger grid size and smaller time step size, and, therefore, prohibitive for completing a simulating a long duration mixing.

The results of this investigation showed that the current storage tank CFD model implemented in the ANSYS Fluent CFD code is capable of successfully reproducing the main features of the jet-ullage interaction in microgravity for two different liquid fill levels in the tank and four different jet flow rates. The focus of the current study was on modeling the fluid flow and interface dynamics. Since modeling the thermal effects of the subcooled jet on the interfacial mass transfer is important, such cases will be considered in future work.

Acknowledgments

This work was supported by the NASA Space Technology Mission Directorate's Technology Demonstration Missions Program under the Evolvable Cryogenics Project.

References

- [1] Kassemi, M, and Chato, D. The Zero Boil-Off Tank Experiment, Cold Facts, Cryogenic Society of America, Vol. 33, Number 3, June, 2017.
- [2] Hirt, C.W., and Nichols B.D., "Volume of fluid (VOF) method for the dynamics of free boundaries," *Journal of Computational Physics*, Vol. 39 No. 1, 1981, pp. 201-225.
- [3] Aydelott, J.C., Modeling of Space Vehicle Propellant Mixing, NASA-TP-2107, January, 1983
- [4] Bentz, M. D., Tank Pressure Control in Low Gravity by Jet Mixing, NASA-CR-191012, March, 1993
- [5] Wendl, M. C., Hochstein, J.I. and Sasmal, G.P. "Modeling of Jet-Induced Geyser Formation in a Reduced Gravity Environment," *AIAA-1991-803*, 1991
- [6] Breisacher K. and Moder, J. "Preliminary Simulations of the Ullage Dynamics in Microgravity during the Jet Mixing Portion of the Tank Pressure Control Experiments," *AIAA 2015-3853, AIAA 50th Joint Propulsion Conference*, AIAA, Orlando, FL, 2015
- [7] O. Kartuzova, M. Kassemi "Modeling Ullage Dynamics of Tank Pressure Control Experiment during Jet Mixing in Microgravity" *52nd AIAA/ASME/SAE/ASEE Joint Propulsion Conference* proceedings, July 2016, Salt Lake City, UT, AIAA2016-4677
- [8] Brigham Young University, "DIPPR 801 Evaluated Process Data," BYU-DIPPR Thermophysical Properties Laboratory, Provo, UT, 2009.
- [9] du Pont de Nemours and Company, "Krytox performance lubricants: Krytox 157 FS Fluorinated Oil," 2000. [Online]. [Accessed 9 September 2009].
- [10] du Pont de Nemours and Company, "DuPont Krytox Performance Lubricants Product Overview," 2002. [Online]. Available: <http://www.vacuumoil.com/msdspdfs/productinfo/krytoxpdf.pdf>. [Accessed 24 May 2013].
- [11] DuPont, "DuPont Krytox Performance Lubricants Product Overview," 2010. [Online]. Available: http://www2.dupont.com/Lubricants/en_US/assets/downloads/H-58505-4_Krytox_Overview_LowRes.pdf. [Accessed 6 March 2014].
- [12] Brackbill J.U., Kothe, D.B., Zemach, C., "A continuum method for modeling surface tension," *J. Comp. Phys.* Vol. 100, 1992, pp. 335-354.
- [13] Menter, F. R., "Two-Equation Eddy-Viscosity Turbulence Models for Engineering Applications," *AIAA Journal*, Vol. 32 No. 8, 1994, pp. 1598-1605
- [14] Wilcox, D.C., *Turbulent Modeling for CFD*, DCW Industries, Inc., La Canada, California, 1998
- [15] Bradshaw, P., Ferriss, D.H., and Atwell, N.P., "Calculation of Boundary-Layer Development Using the Turbulent Energy Equation," *Journal of Fluid Mechanics*, Vol. 28, No. 3, 1967, pp. 593-616.
- [16] F.Nicoud and F.Ducros "Subgrid-Scale Stress Modelling Based on the Square of the Velocity Gradient Tensor." *Flow, Turbulence, and Combustion*, 62(3):183-200, 1999.
- [17] ANSYS Fluent Documentation. Release 19.2. September 2018.

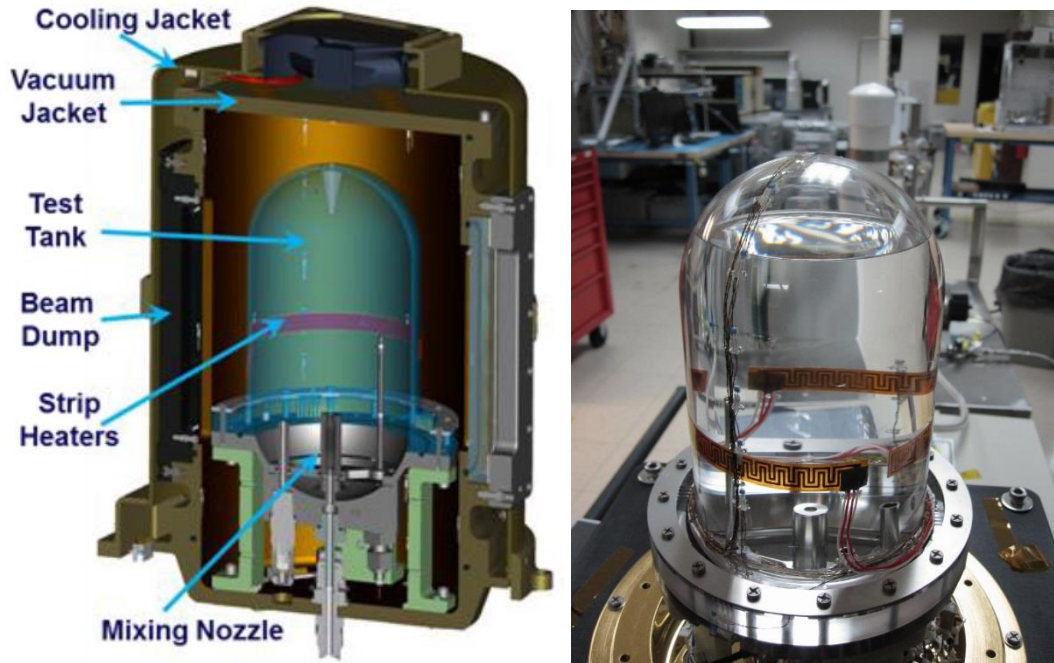


Fig. 1 ZBOT experimental setup.

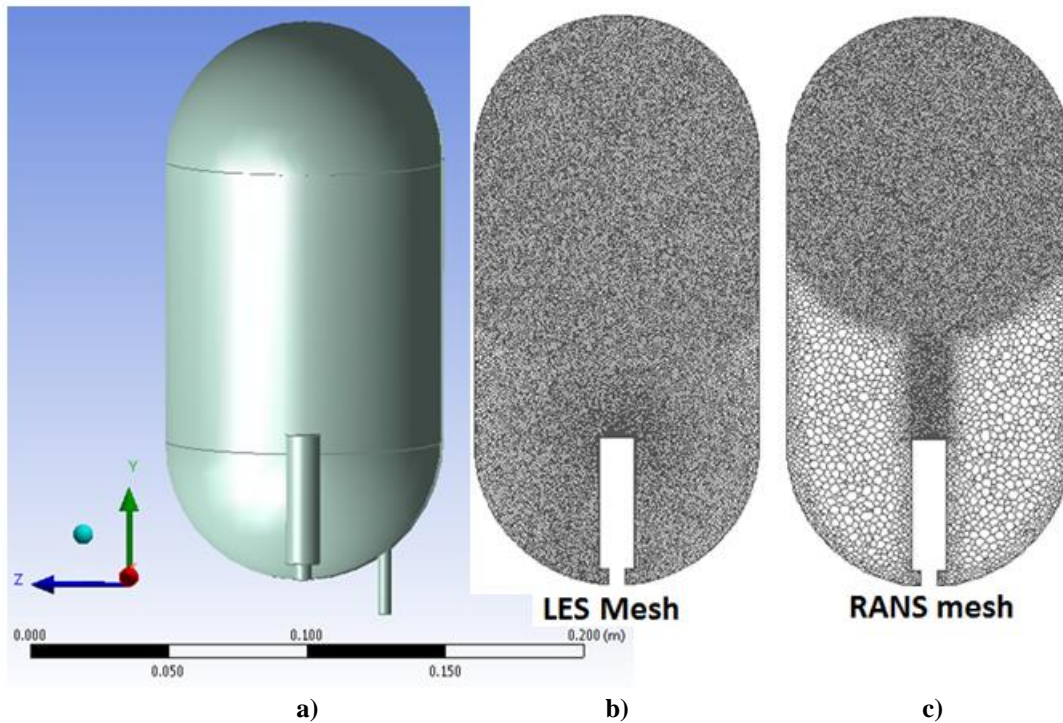


Fig. 2 ZBOT geometry - (a) and computational meshes (LES (13 mln. cells - (b)) and RANS (6 mln. cells - (c)) used for modeling.

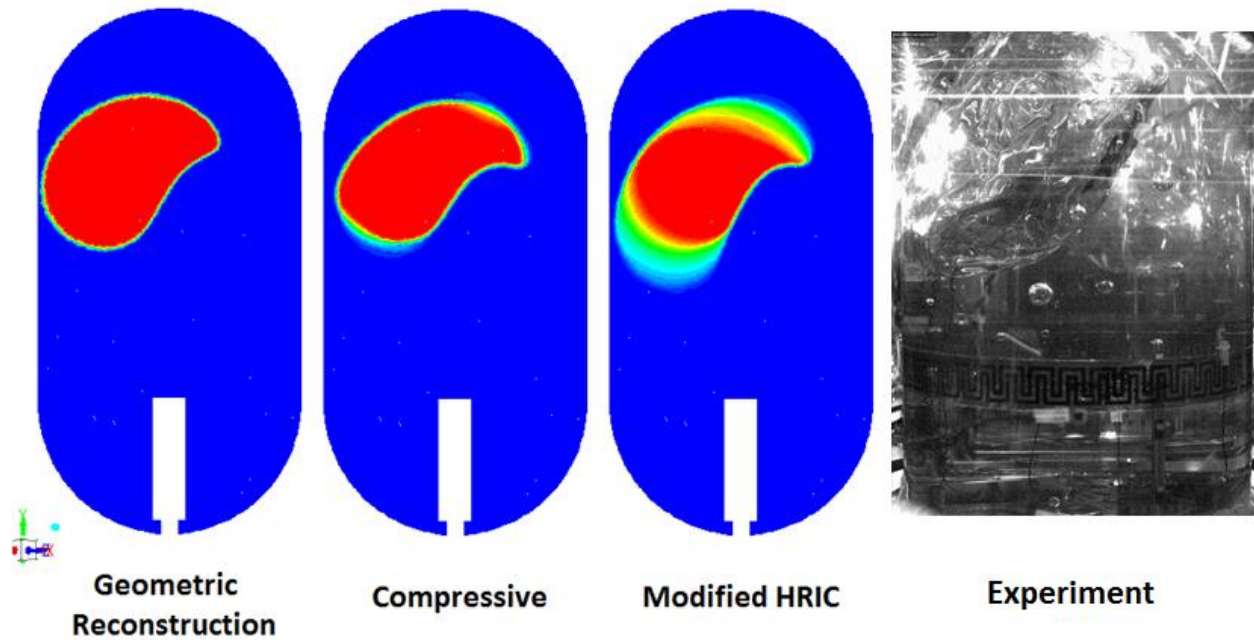


Fig. 3 Effect of volume fraction equation discretization scheme on ullage shape and interface sharpness with RANS turbulence model (ZBOT Case 256), [V*1].

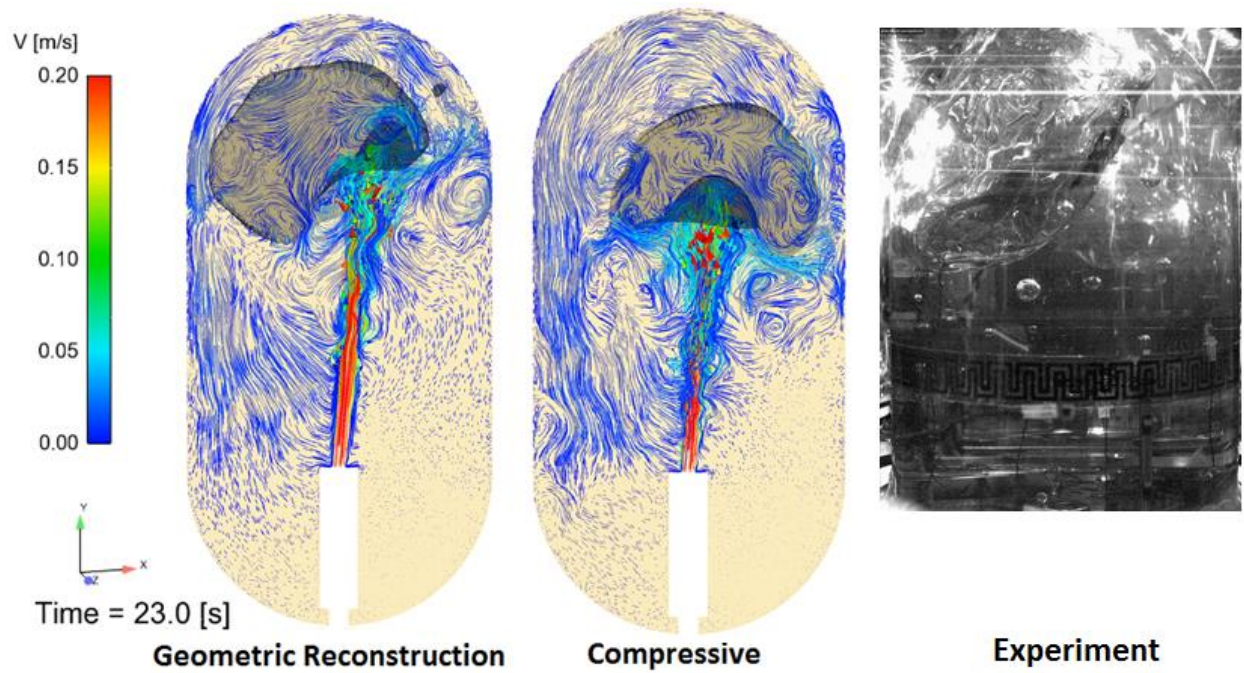


Fig. 4 Effect of volume fraction equation discretization scheme on ullage shape and interface sharpness with LES turbulence model (ZBOT Case 256), [V*1].

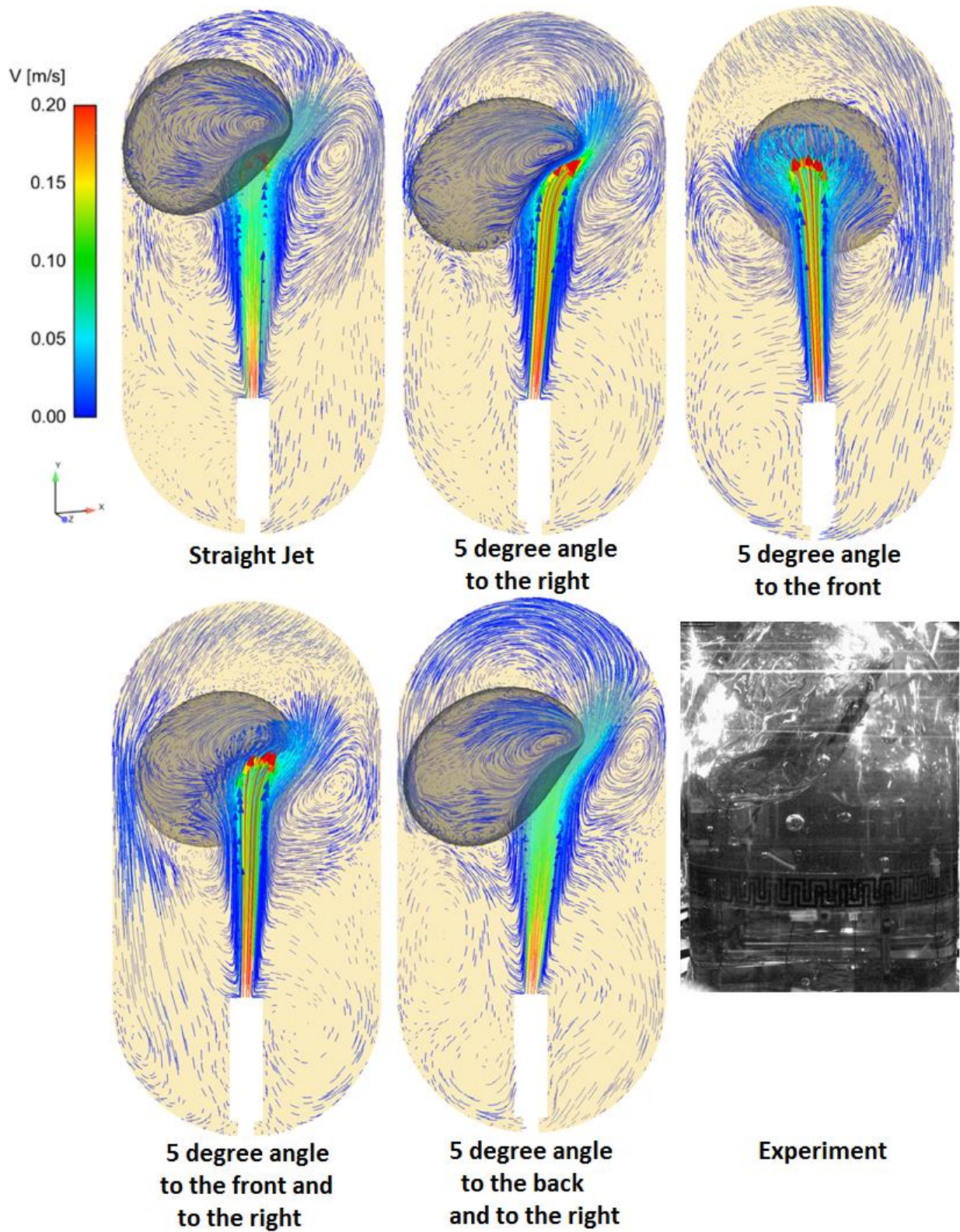


Fig. 5 Effect of jet angle: straight jet compared to different jet orientations at 119 seconds of mixing and to the experiment (ZBOT Case 256), [V^*1].

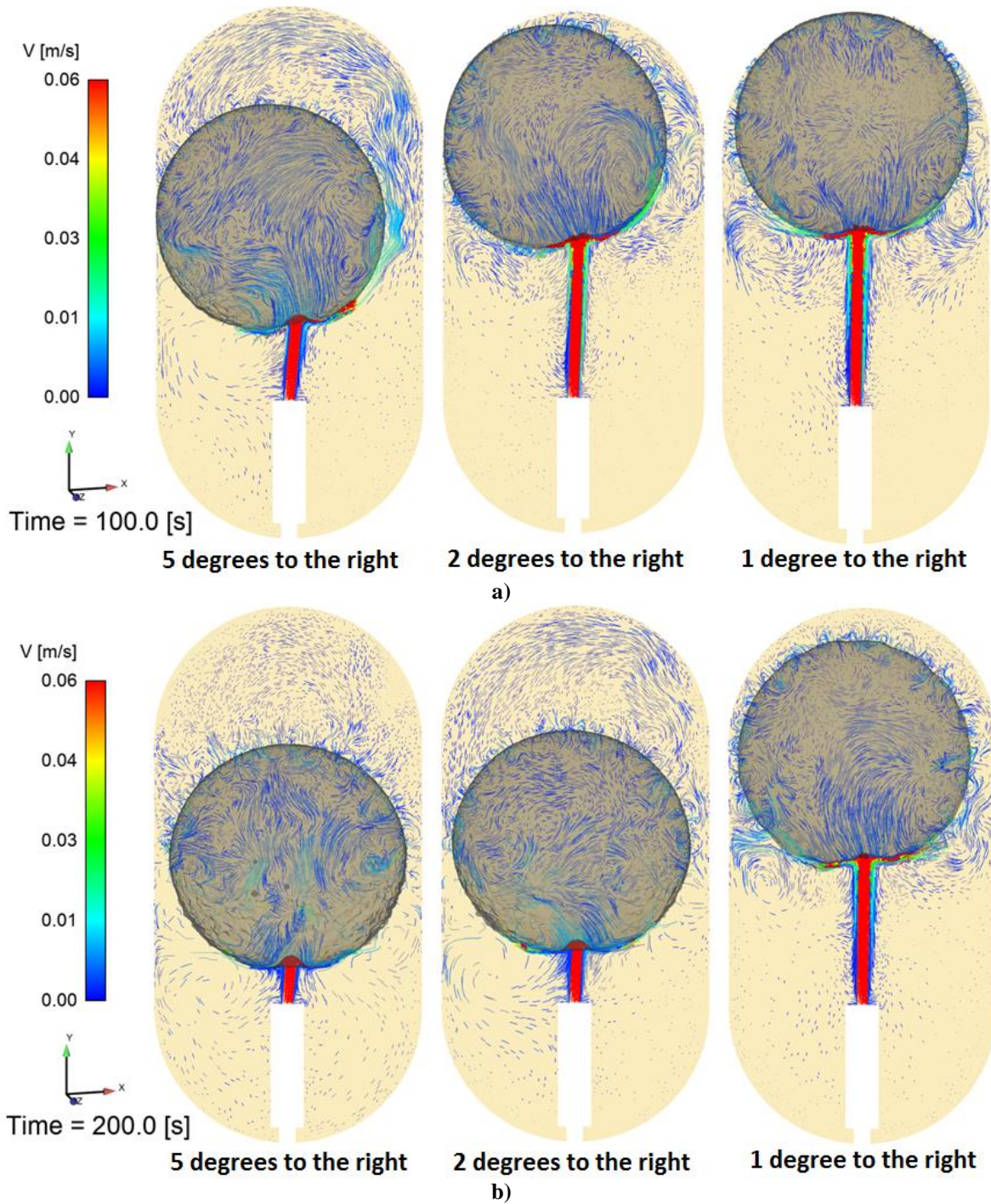


Fig. 6 Effect of the jet angle value: 5 degrees to the right (left), 2 degrees to the right (middle) and 1 degree to the right (right) at 100 seconds - (a) and 200 seconds of mixing - (b) (ZBOT Case 9), [V*1.35].

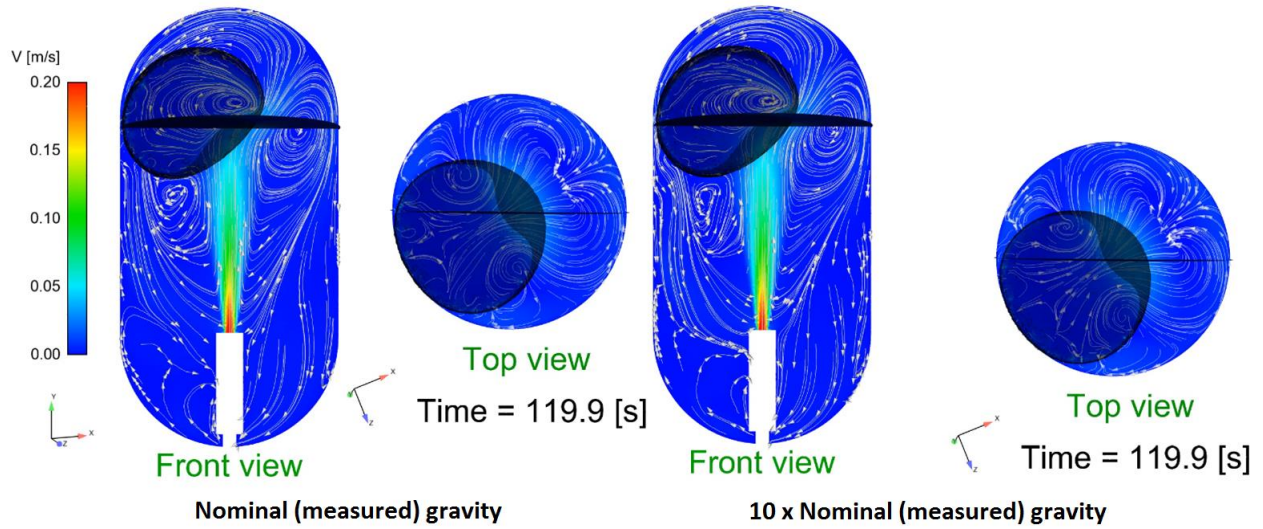


Fig. 7 Effect of the value of the gravitational acceleration in the axial direction: Nominal (measured) (left) and 10 x Nominal value (right) (ZBOT Case 256), [V*1].

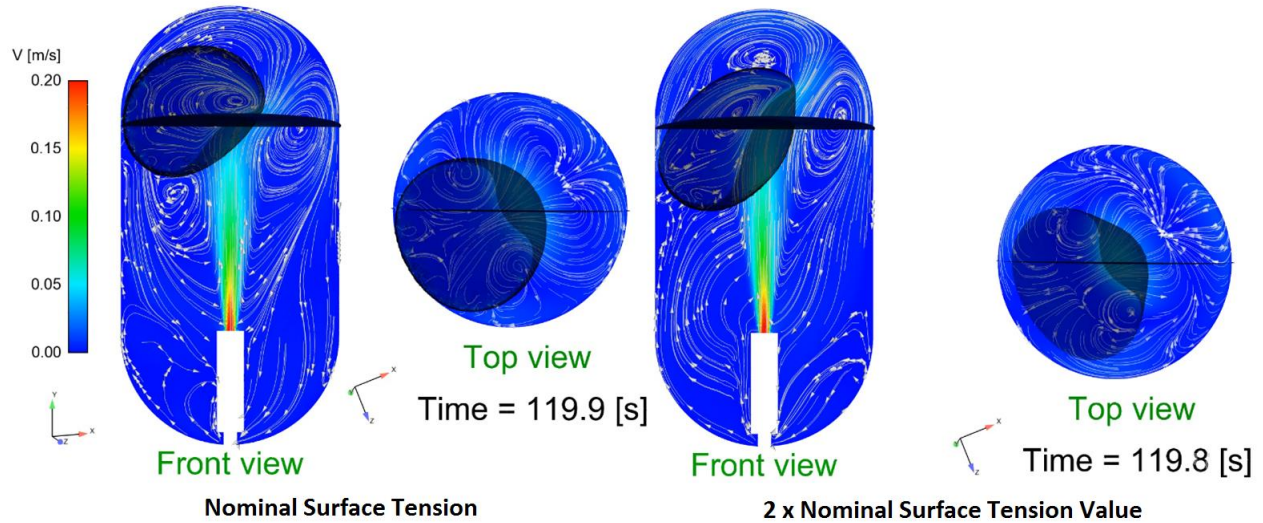


Fig. 8 Effect of the value of the surface tension: Nominal (measured) (left) and 2 x Nominal value (right) (ZBOT Case 256), [V*1].

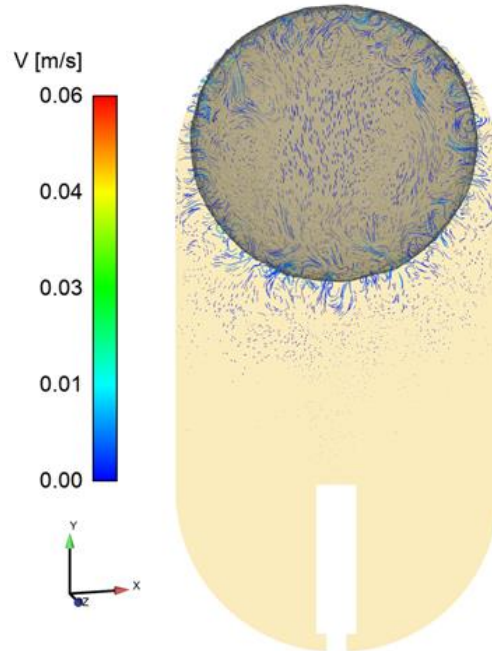


Fig. 9 ZBOT Case 9 (70% fill level, 6 cm/s jet speed) – Initial ullage position.

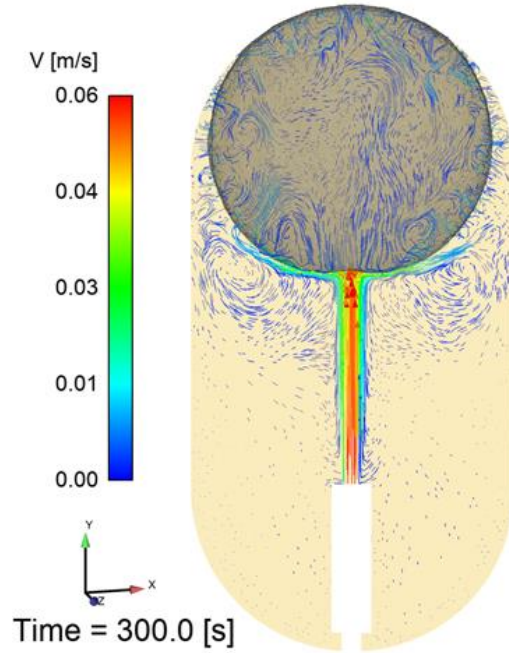


Fig. 10 ZBOT Case 9 (70% fill level, 6 cm/s jet speed) – Final ullage position – straight jet, [V*1].

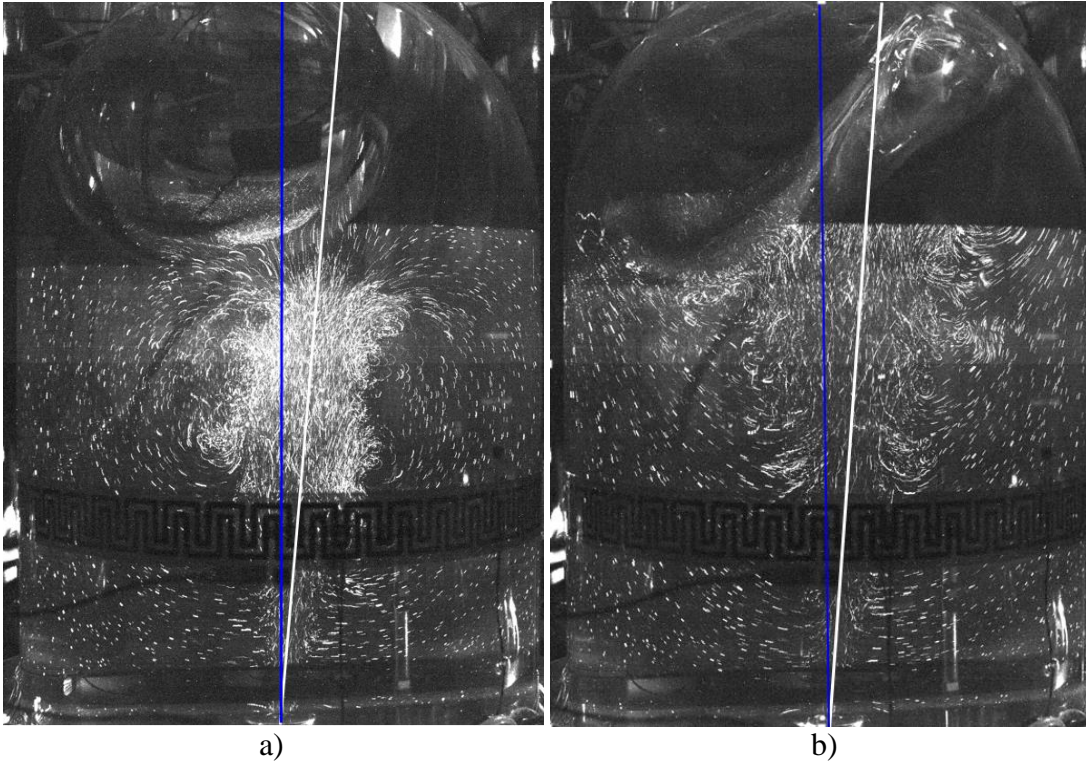


Fig. 11 Flow visualization with DPIV particle streaks: ZBOT DPIV Case 500 (20 cm/s jet speed). Tank centerline (blue) and Jet centerline (white) are shown.

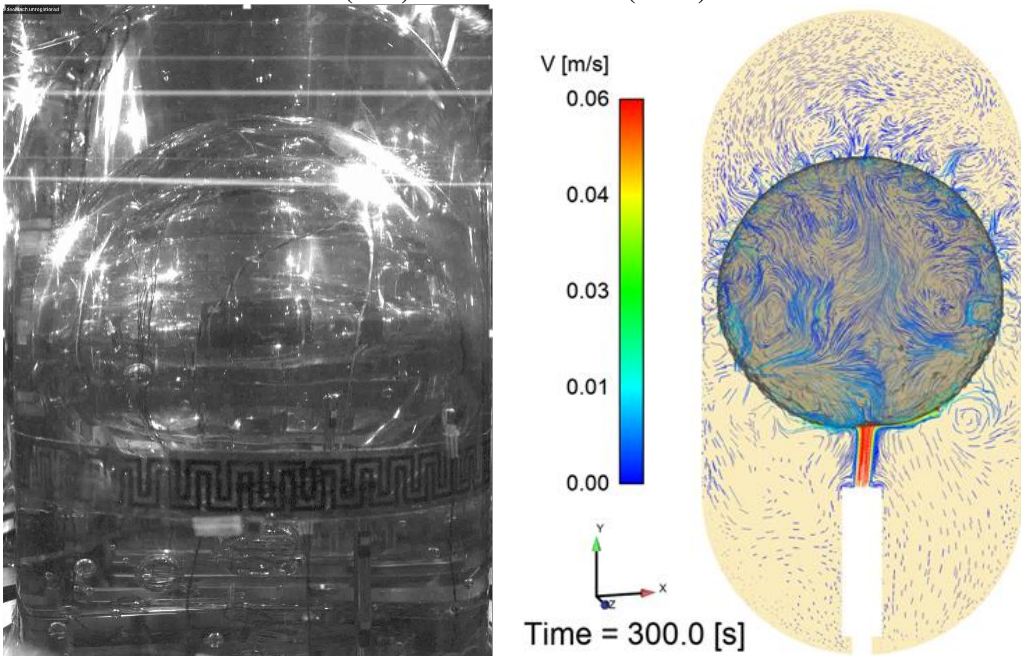


Fig. 12 ZBOT Case 9 (70% fill level, 6 cm/s jet speed) – Final ullage position – 5 deg. to the right jet angle, [V*1].

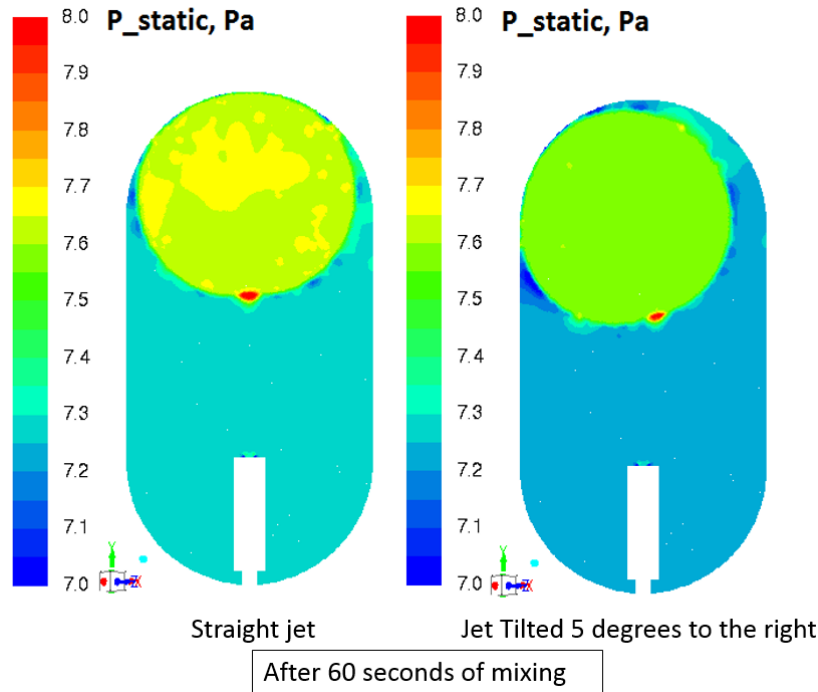


Fig. 13 ZBOT Case 9 (70% fill level, 6 cm/s jet speed) – Pressure contours at the tank center plane – 5 deg. jet angle to the right vs. straight jet, [V*1].

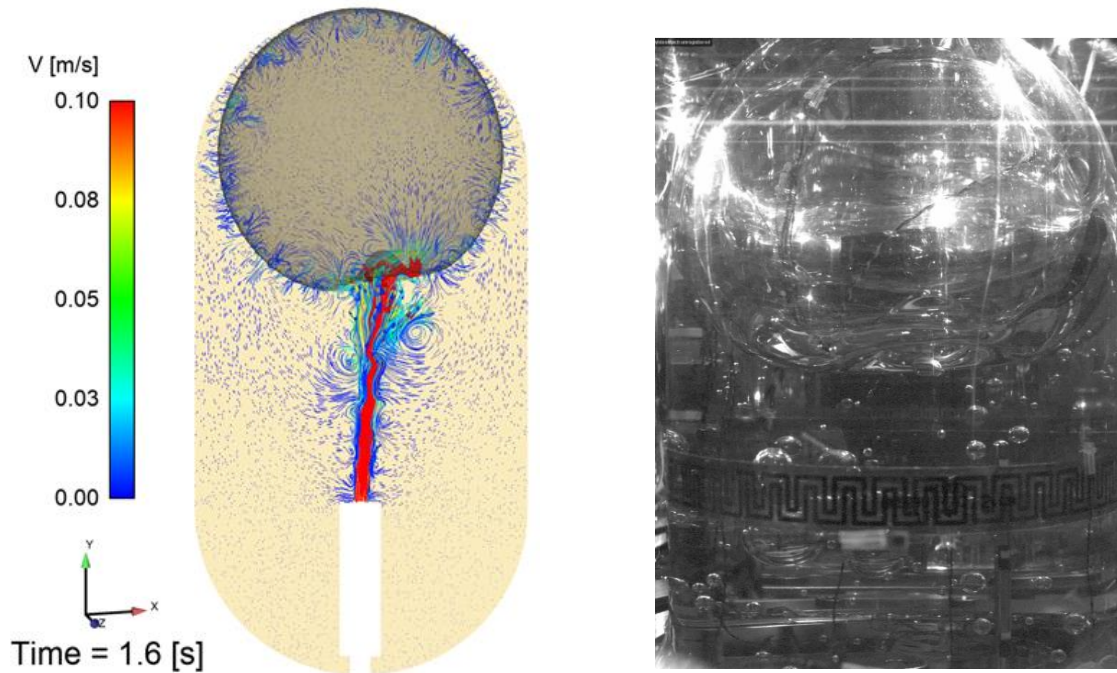


Fig. 14 ZBOT Case 24 (70% fill level, 10 cm/s jet speed) - Ullage location and curved vectors from the CFD LES case (left) and white light image from the experiment (right) after 1.6 seconds of mixing, [V*1.35].

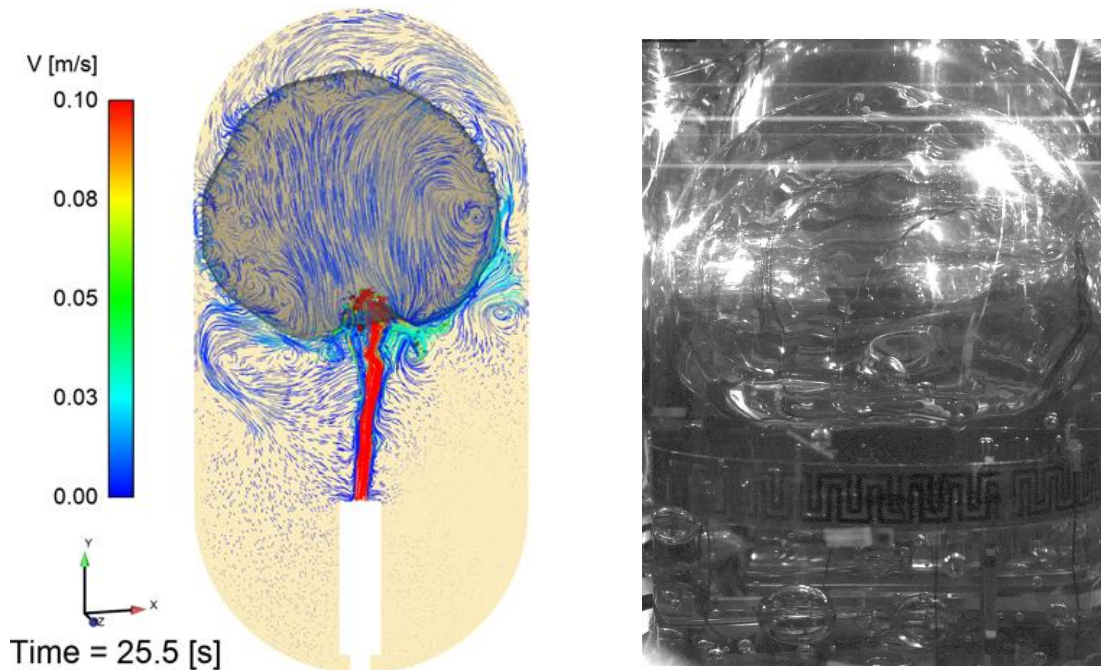


Fig. 15 ZBOT Case 24 (70% fill level, 10 cm/s jet speed) - Ullage location and curved vectors from the CFD LES case (left) and white light image from the experiment (right) after 25.5 seconds of mixing, [V*1.35].

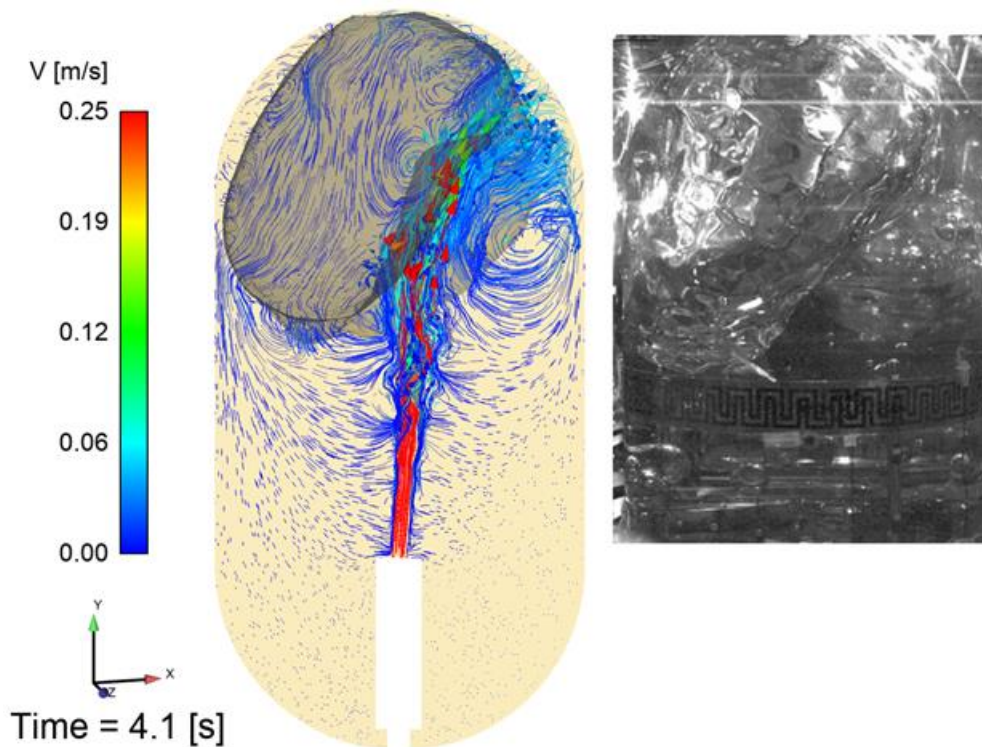


Fig. 16 ZBOT Case 27 (70% fill level, 25 cm/s jet speed) - Ullage location and curved vectors from the CFD LES (5 degrees jet angle to the right) case (left), and white light image from the experiment (right) after 4 seconds of mixing, [V*1.35].

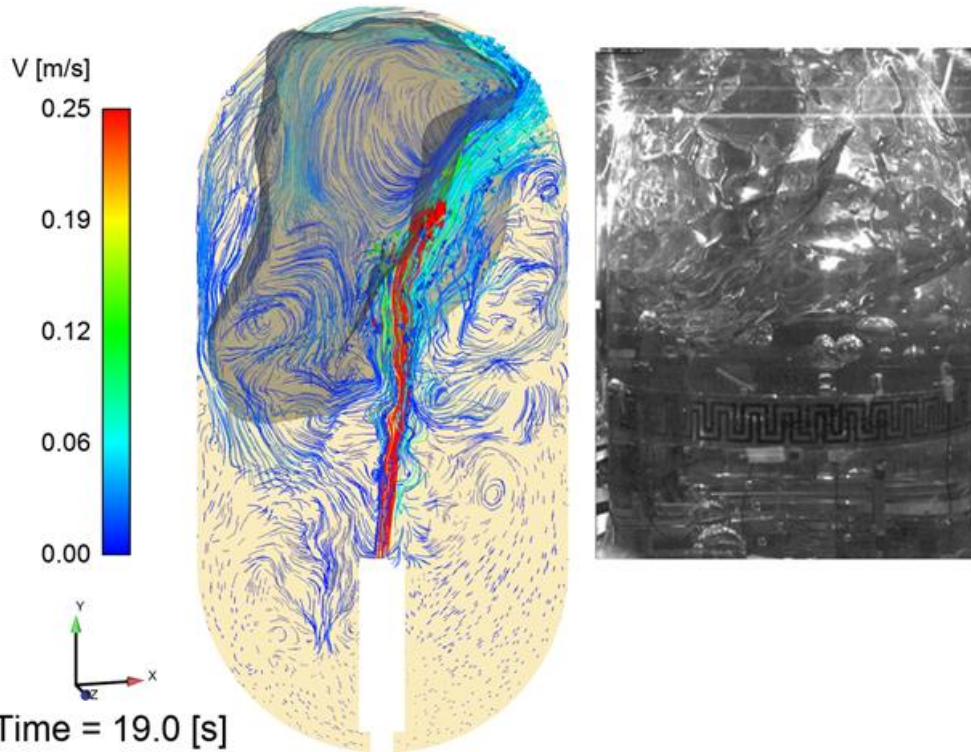


Fig. 17 ZBOT Case 27 (70% fill level, 25 cm/s jet speed) - Ullage location and curved vectors from the CFD LES (5 degrees jet angle to the right) case (left), and white light image from the experiment (right) after 19 seconds of mixing, [V*1.35].

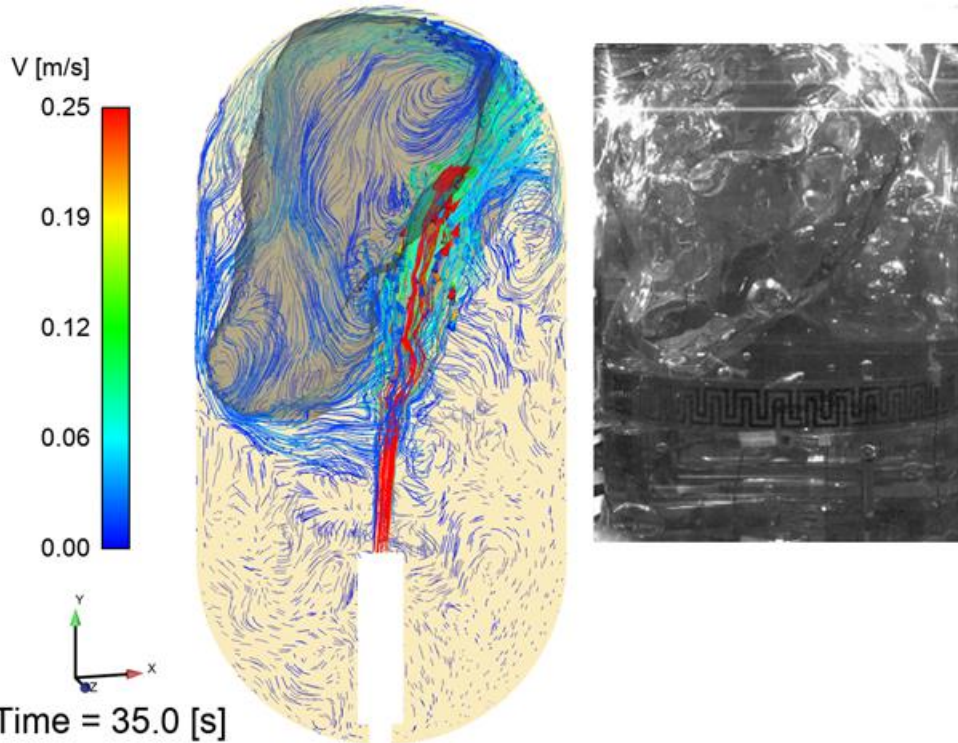


Fig. 18 ZBOT Case 27 (70% fill level, 25 cm/s jet speed) - Ullage location and curved vectors from the CFD LES (5 degrees jet angle to the right) case (left), and white light image from the experiment (right) after 35 seconds of mixing, [V*1.35].

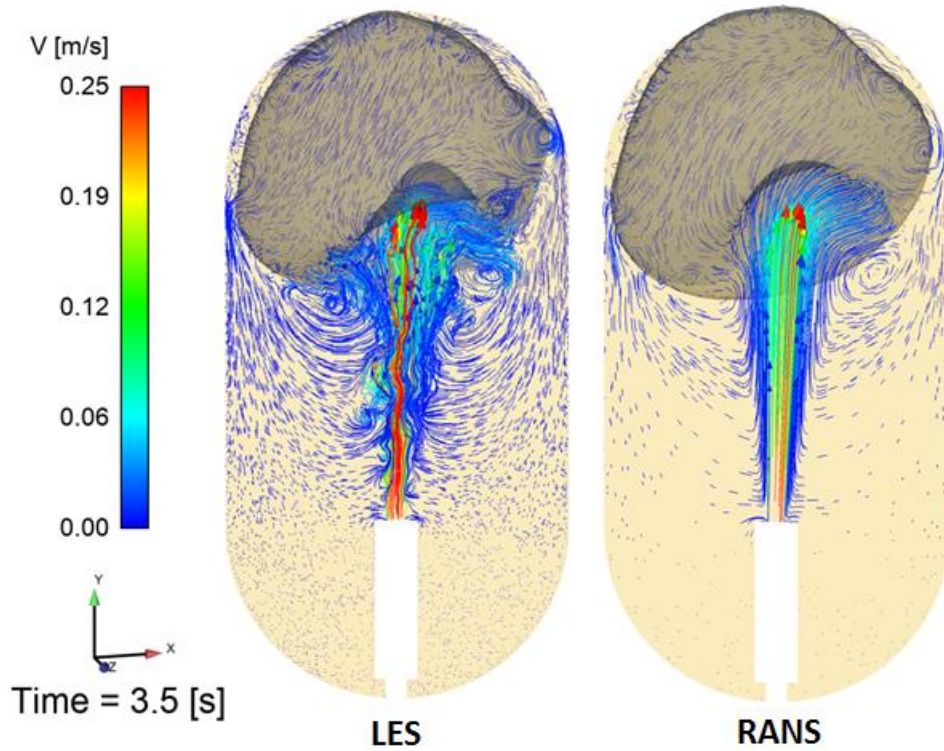


Fig. 19 ZBOT Case 27 (70% fill level, 25 cm/s jet speed) - Ullage location and curved vectors from the CFD LES case (left) and RANS (right) after 3.5 seconds of mixing, [Vx1].

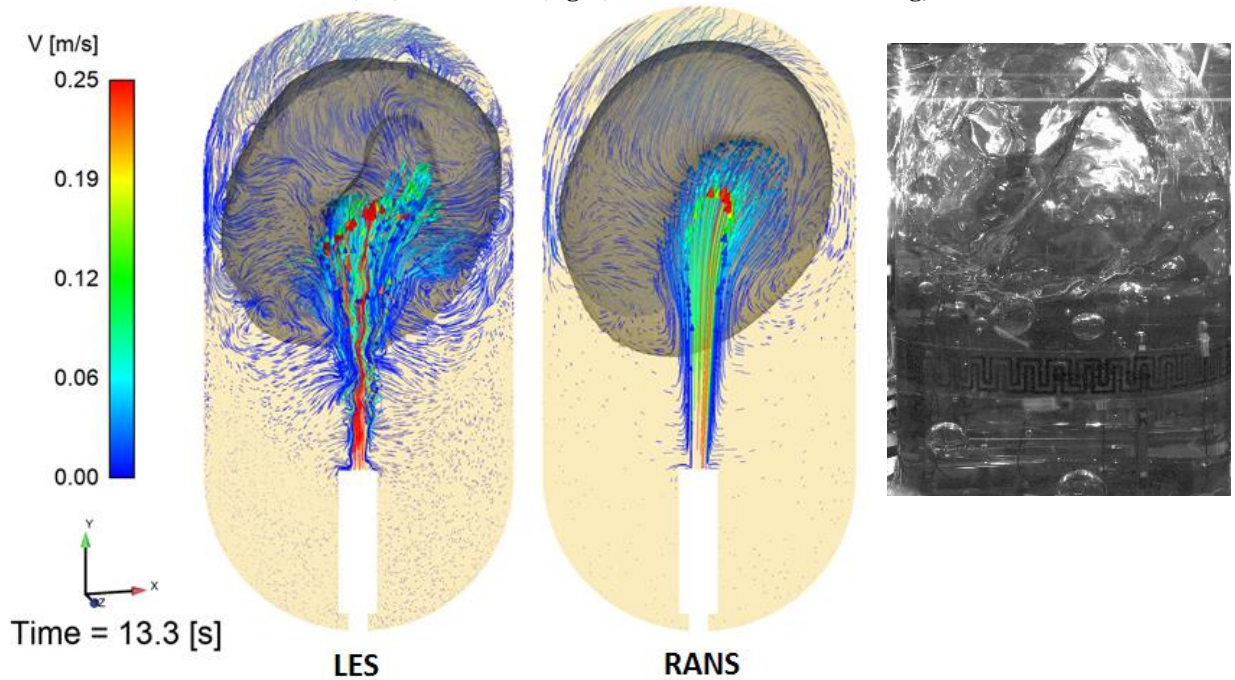


Fig. 20 ZBOT Case 27 (70% fill level, 25 cm/s jet speed) - Ullage location and curved vectors from the CFD LES case (left) and RANS (middle) compared with the experiment (right) after 13.3 seconds of mixing, [Vx1].

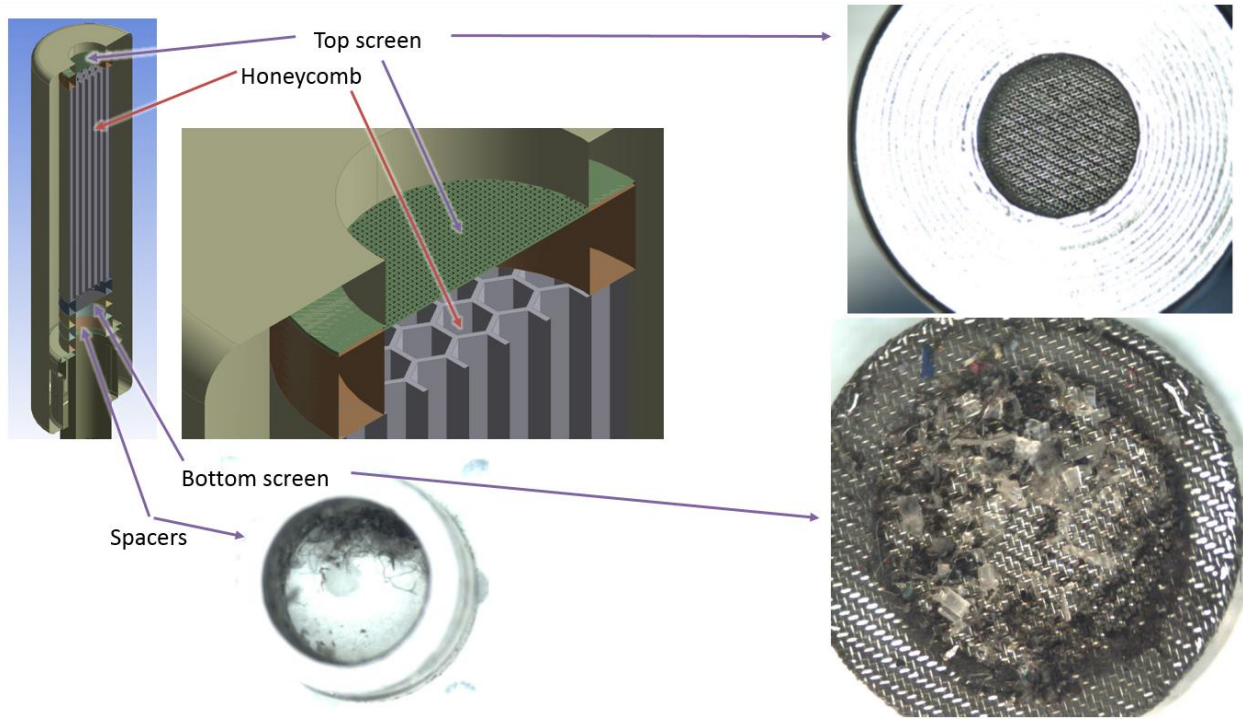


Fig. 21 Nozzle configuration and screen blockage discovered after disassembly.

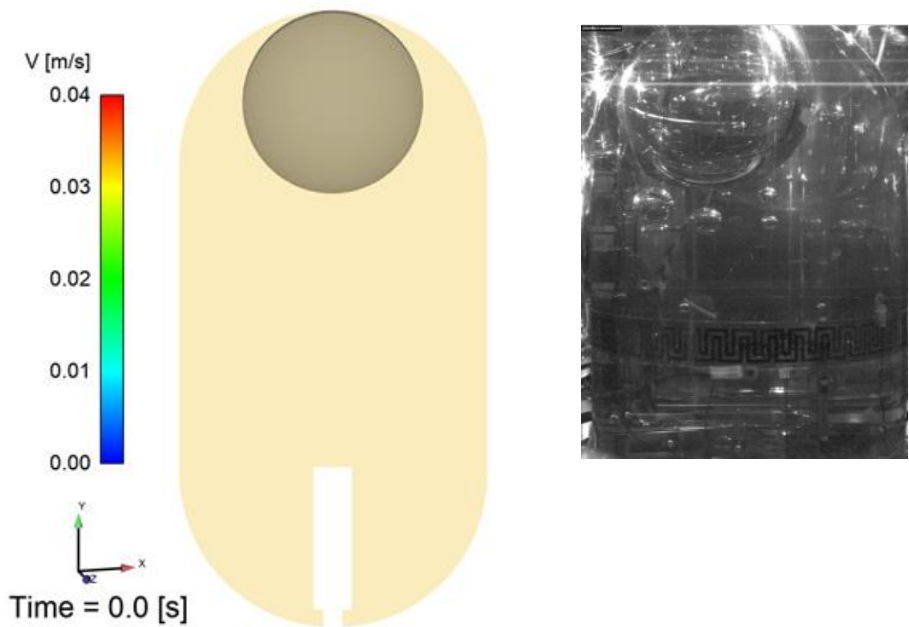


Fig. 22 ZBOT Case 260 (90% fill level, 4 cm/s jet speed) - Initial ullage position from CFD (left) and from experiment (right).

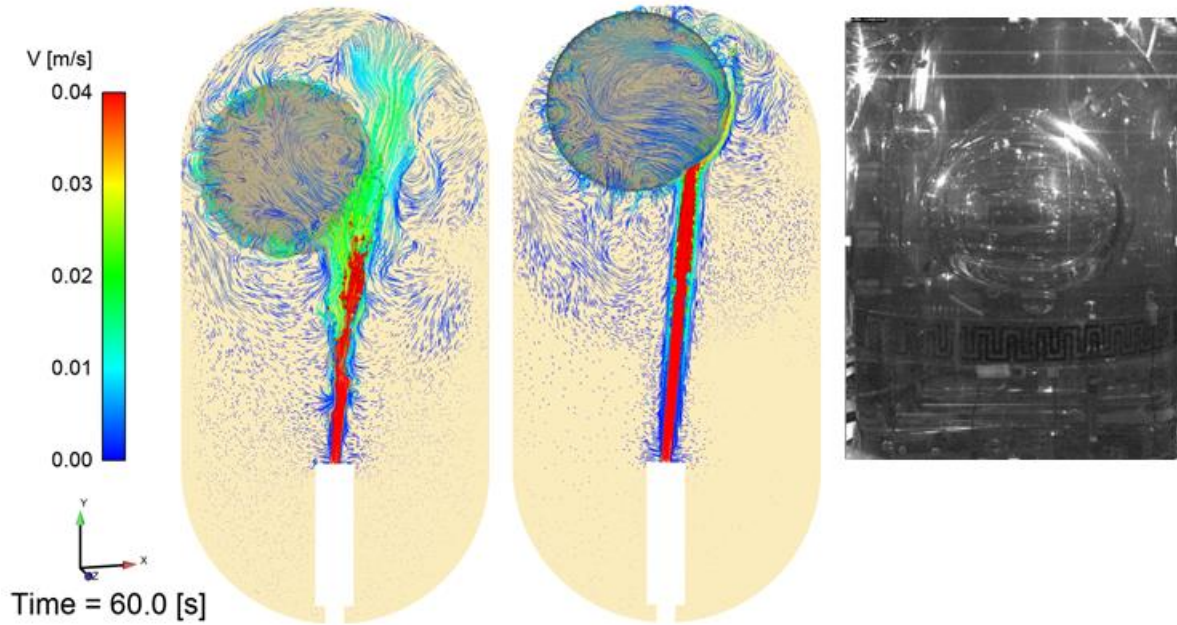


Fig. 23 ZBOT Case 260 (90% fill level, 4 cm/s jet speed) - Ullage position from CFD LES (left); CFD Laminar (middle); and from experiment (right) after 60 seconds of mixing, [V*2].

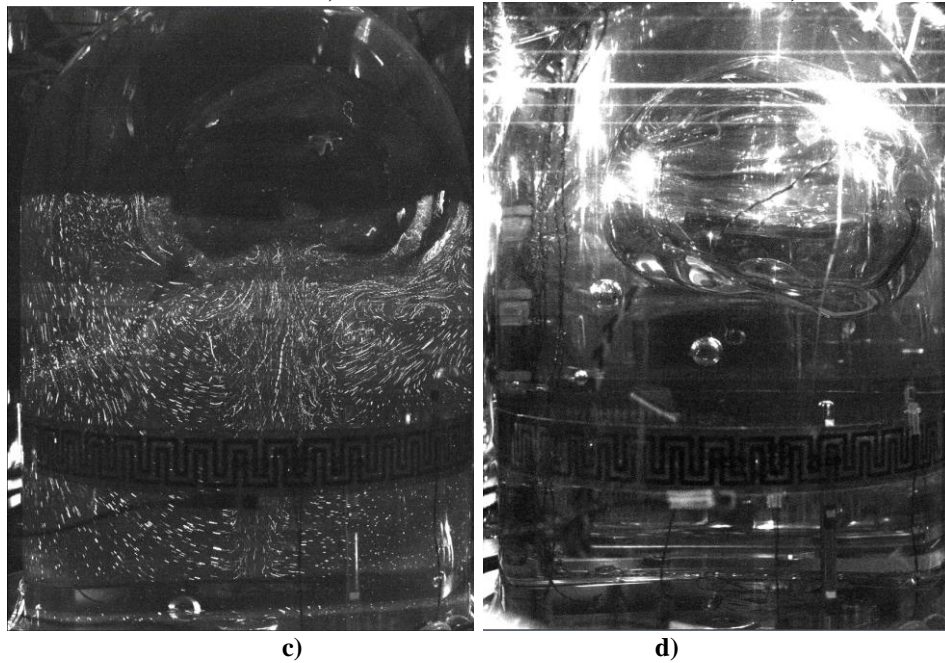
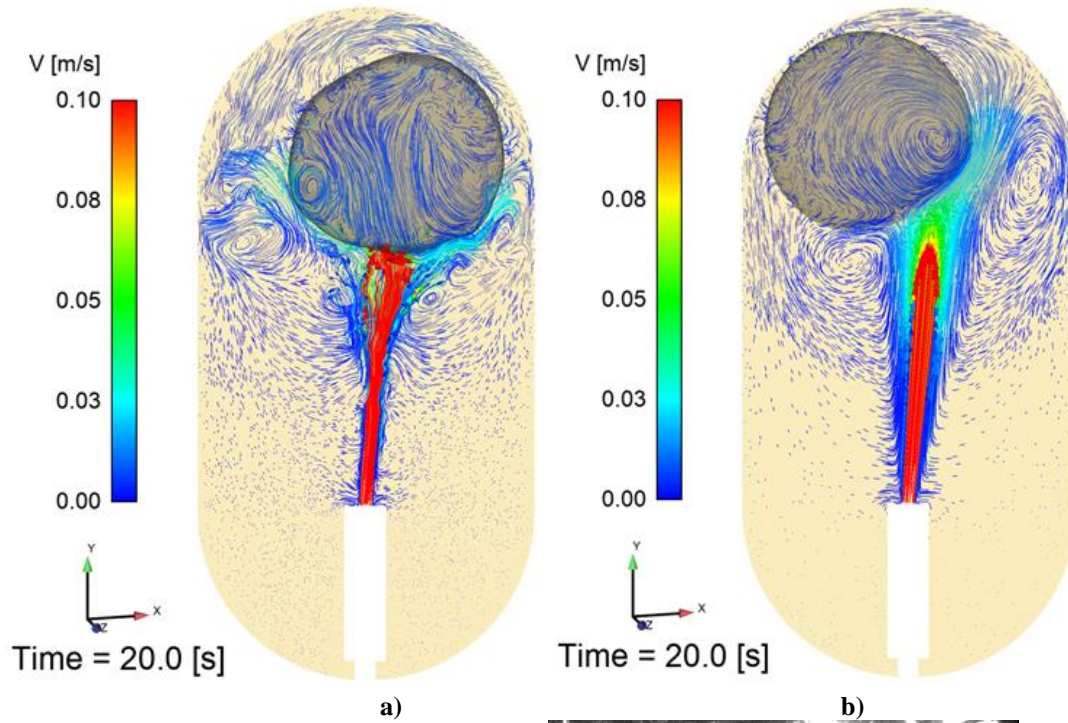


Fig. 24 ZBOT Case 254 (90% fill level, 10 cm/s jet speed) - Ullage position and curved vectors from CFD LES-(a) and from CFD RANS-(b); flow visualization using streaks from experiment-(c) and ullage position from experiment-(d) after 20 seconds of mixing, [V*1.35].

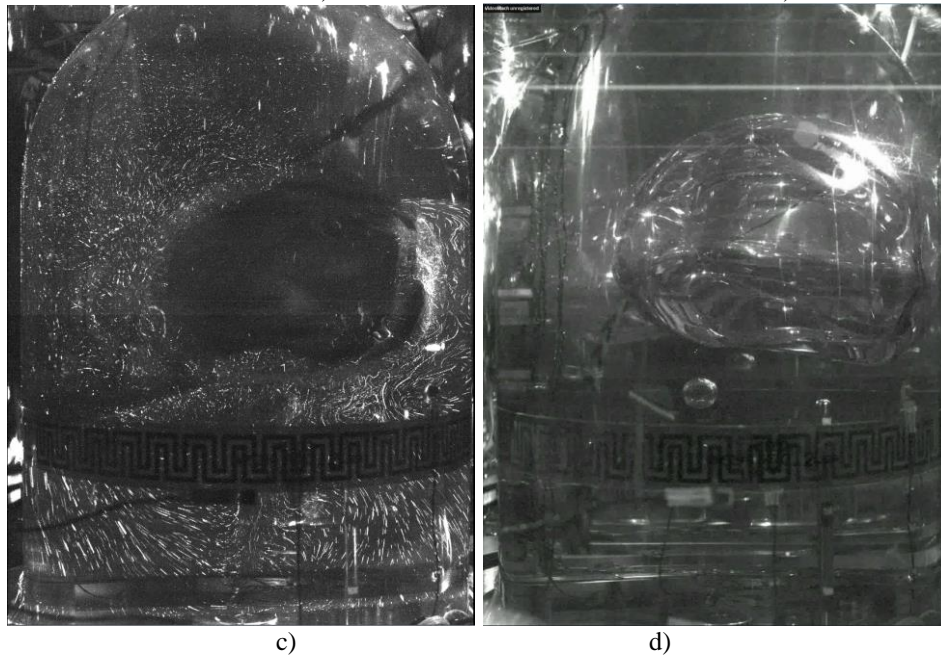
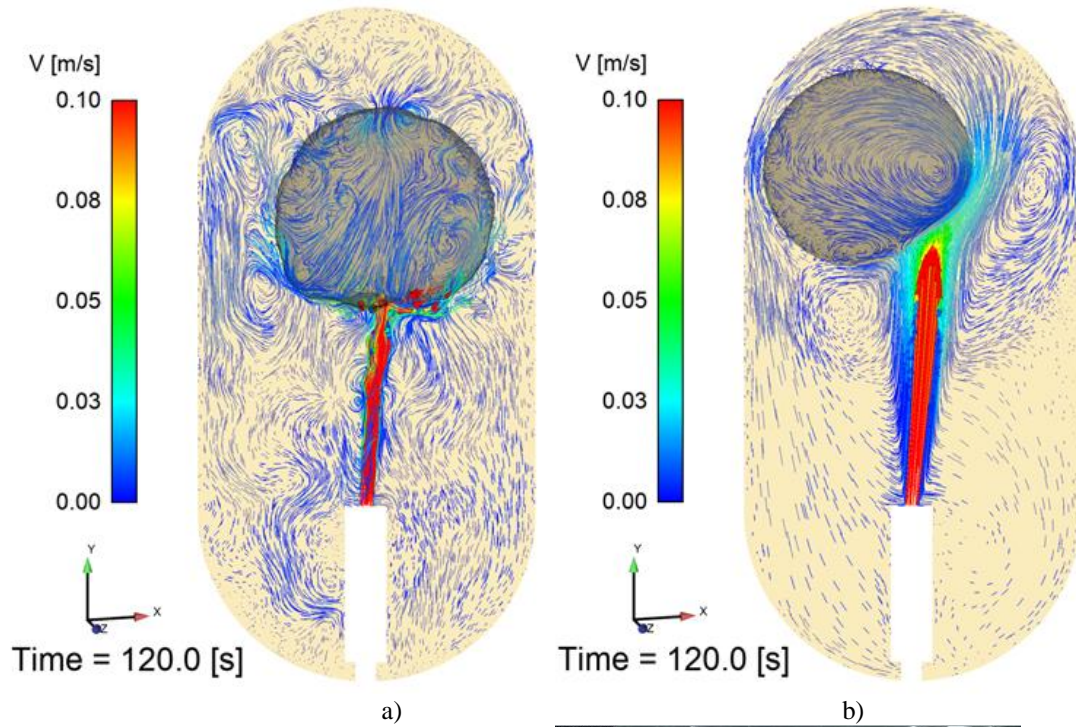


Fig. 25 ZBOT Case 254 (90% fill level, 10 cm/s jet speed) - Ullage position and curved vectors from CFD LES-(a) and from CFD RANS-(b); flow visualization using streaks from experiment-(c) and ullage position from experiment-(d) after 120 seconds of mixing, $[V*1.35]$.

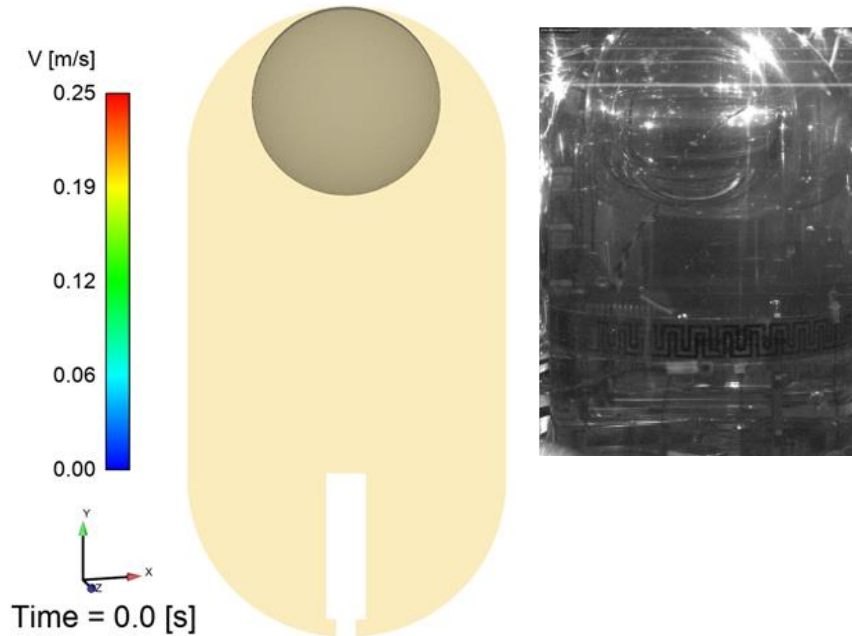


Fig. 26 ZBOT Case 258 (90% fill level, 25 cm/s jet speed) - Initial ullage position from CFD (left) and from experiment (right).

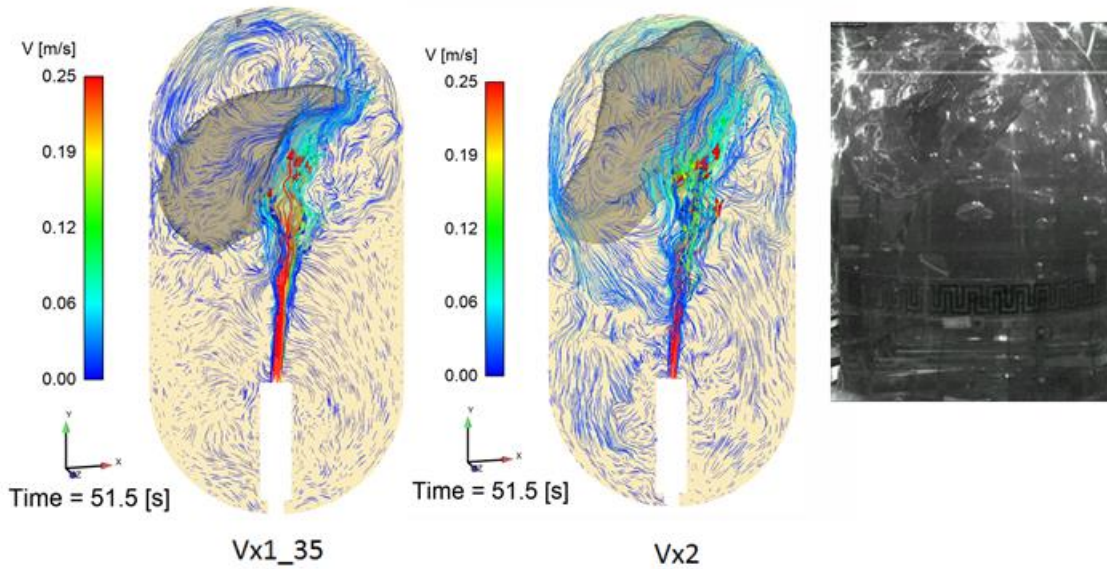


Figure 27: ZBOT Case 258 (90% fill level, 25 cm/s jet speed) - Ullage position from CFD LES V*1.35 (left); CFD LES V*2 (middle); and from experiment (right) after 51.5 seconds of mixing